Final Report for 2025 SCEC Grant 25053

The interplay of seismic and aseismic fault slip during earthquake swarms in California and Nevada

Daniel T. Trugman[1], and Yu Jiang[1]

[1]Nevada Seismological Laboratory, University of Nevada, Reno, NV 89557

Objectives

The primary objective of this project is to integrate seismicity rate observations with surface deformation measurements to improve our understanding of aseismic fault behavior during earthquake swarms. By jointly analyzing these complementary datasets, the project aims to better constrain the physical processes that precede and accompany swarm activity and, in some cases, lead to large mainshocks. This work directly supports the Statewide California Earthquake Center (SCEC) Earthquake System Science priority of advancing predictive analyses of seismicity, helping to shift earthquake science from a largely post-event response toward more proactive, pre-earthquake assessment.

A key outcome of the project is the development of *T-rate*, a Python-based Bayesian inversion framework that estimates the temporal history of stress changes directly from seismicity rate observations. The *T-rate* methodology has been rigorously validated through synthetic experiments and applied to real earthquake swarms in California and Nevada to infer stress evolution during swarms. This new tool provides a simple yet robust approach for investigating fault slip evolution and its interaction with seismicity. Beyond earthquake swarms, the *T-rate* framework offers broader applicability to other frictionally driven processes, including subduction zone slow slip events, landslides, and surging glaciers. A manuscript describing the *T-rate* inversion framework, with an example application to the 2008 Reno-Mogul earthquake swarm has been submitted and is currently under review.

Methodology

We propose a new mathematical framework that directly links seismicity rate to stress rate, building on the generalized approach by Heimisson & Segall (2018). Instead of assuming an instantaneous jump as in J. Dieterich (1994) and a constant stressing rate as in Segall et al. (2006), we adopt a more flexible parameterization in which the stress rate, $\mathrm{d}\Delta S(t)/\mathrm{dt}$, is represented by a trapezoidal function. This formulation allows the stressing rate to gradually increase over time, then remain steady over a finite interval, and finally decrease back to zero over time, thereby capturing realistic transient loading processes.

Given the parameterized stress-rate history, we derive a closed-form solution for the normalized seismicity rate, $R(t)/r$, which serves as the forward model. We embed this forward model within a Bayesian inverse framework to infer the temporal evolution of stress directly from earthquake catalogs, even in regions where geodetic observations are sparse or unavailable. Posterior probability distributions of the optimal model parameters are estimated using Markov chain Monte Carlo sampling, from which parameter estimates and associated uncertainties are

obtained using PyMC software (Abril-Pla et al., 2023). Given the discrete and count-based nature of earthquake occurrence, we model the observed seismicity using a Poisson likelihood function. As illustrated in Figure 1, this inversion framework robustly recovers stress-rate histories in synthetic experiments.

We evaluate the robustness and sensitivity of the workflow systematically through comprehensive synthetic experiments. The synthetic tests demonstrate that the inferred stress evolution is generally robust to the choice of prior distributions, noise levels, and sampling algorithms. In contrast, the likelihood formulation and the functional representation of the stress rate play a critical role in accurate parameter reconstruction. Overall, the combination of a Poisson likelihood and a flexible trapezoidal-based stress-rate formulation provides the most physically consistent and statistically reliable description of stress evolution.

We also find that the estimation of stress amplitude is significantly improved when parameterizing the model in terms of $t_a\dot{\tau}_r$ rather than $A\sigma_0$. While $A\sigma_0$ has been commonly adopted in previous forward and inverse studies, both A and σ_0 are poorly constrained in natural earthquake sequences. In contrast, t_a is explicitly included as a model parameter, and $\dot{\tau}_r$ can be independently estimated from regional or global strain-rate models derived from geodetic observations. By incorporating these external constraints, the trade-off between stress amplitude and frictional resistance is substantially reduced, leading to a more accurate and stable inversion.

Results

After validating the robustness of the method using synthetic experiments, we apply the workflow to eight earthquake swarms in California (CA) and Nevada (NV): 2008 Reno-Mogul (NV), 2011 Hawthorne (NV), 2012 Brawley (CA), 2014-2018 Sheldon (NV), 2015 San Ramon (CA), 2016 Nine Mile Ranch (NV), 2020 Maacama (CA), and 2020 Westmorland (CA).

We first conduct a detailed analysis of the 2008 Reno-Mogul swarm. To assess whether processes beyond earthquake-earthquake triggering contribute to the early evolution of the swarm, we first decluster the earthquake catalog to remove seismicity rate changes driven primarily by aftershock triggering. This procedure allows us to isolate seismicity potentially driven by aseismic fault slip. After removing aftershocks associated with earthquake triggering, we estimate a transient, non-earthquake-triggered seismicity rate, R (Zaliapin & Ben-Zion, 2013). The long-term background seismicity rate, r, is estimated independently using the stochastic declustering framework of Zaliapin & Ben-Zion (2020). The resulting ratio R/r serves as the observable input for our Bayesian stress-evolution inversion. Figure 2 shows the observed and modeled R/r for the 2008 Mogul-Reno swarm, together with the inferred stress-rate and cumulative stress histories. The preferred model reveals three distinct phases of elevated stress rate. The first phase begins on February 12, with a peak stress rate of 0.003 ± 0.0005 MPa/day since April 13. The second phase spans March 25 to April 15, with a peak stress rate of 0.09 ± 0.02 MPa/day between April 2 and April 10. The third phase spans April 15 to April 25, during which the stress rate reaches its maximum of 0.5 ± 0.3 MPa/day on April 25, one day before the M 5.1 event.

We then apply the same workflow to seven additional earthquake swarms listed in the proposal and examine whether aseismic fault slip signals can be inferred from seismicity rates. Based on the presence or absence of a measurable increase in non-earthquake-triggered seismicity prior to

the largest event, the swarms can be broadly divided into two categories: (1) swarms that show no clear evidence of non-earthquake-triggered seismicity before the most energetic event, including 2016 Nine Mile Ranch, and 2020 Maacama; and (2) swarms that exhibit a clear increase in non-earthquake-triggered seismicity prior to the main event. The latter category includes 2008 Reno-Mogul, 2011 Hawthorne, 2012 Brawley, 2015 San Ramon, 2014-2018 Sheldon, and 2020 Westmorland swarms.

For swarms exhibiting clear non-earthquake-triggered seismicity, we performed stress-rate inversions using the observed R/r time series and compared the inferred stress-loading phases with independently observed surface deformation signals derived from GPS and InSAR measurements. Figure 3 shows the continuous GPS time series recorded during the Reno-Mogul earthquake swarm. Clear deformation signals occurred 3-4 days before the M 5.1 earthquake on April 26, particularly at stations RENO (North component), VRDE (East, North, and Vertical components), and MOGL (North and Vertical components). The observed displacements reach amplitudes of 1-3 cm and are observed in both 5-minute and daily solutions. These signals represent independent geodetic evidence that the fault was slipping aseismically in the 3-4 days leading up to the M 5.1 earthquake. For the 2012 Brawley and 2020 Westmorland swarms, the stress changes began approximately 10-15 hours before the largest event, reaching a cumulative stress increase of 0.6-0.8 MPa one hour prior to the mainshock. For the 2020 Westmorland swarm, this pattern is consistent with independent high-rate GPS observations, which detected the onset of transient aseismic deformation 2-15 hours before the initiation of seismicity, indicating a precursory slow slip event (Sirorattanakul et al., 2022).

Future work

The results obtained over the past year have laid a strong foundation for further exploration of stress changes inferred from seismicity rate variations. Part of this work were presented at the SSA Annual Meeting in April 2025 and the SCEC Annual Meeting in September 2025, where we received constructive and insightful feedback on multiple aspects of the methodology and interpretation. We plan to present the complete study at the SSA Annual Meeting in April 2026. The newly developed method, *T-rate*, which estimates stress-rate evolution directly from seismicity rate changes, has been submitted to *JGR: Solid Earth* and is currently under review.

Beyond applications to natural earthquake swarms, an important direction of future work is to extend this framework to laboratory-based earthquake experiments. In such experiments, acoustic emission (AE) events serve as analogs for seismicity and provide high-resolution observations of nucleation and failure processes. A key advantage of laboratory AE datasets is the availability of independently measured, time-dependent stress evolution, which serves as a known ground truth. This allows for a direct and quantitative validation of the stress-rate estimates inferred from AE event rates using the *T-rate* framework. Successful validation in controlled laboratory settings will strengthen confidence in the method and support its broader application to natural fault systems.

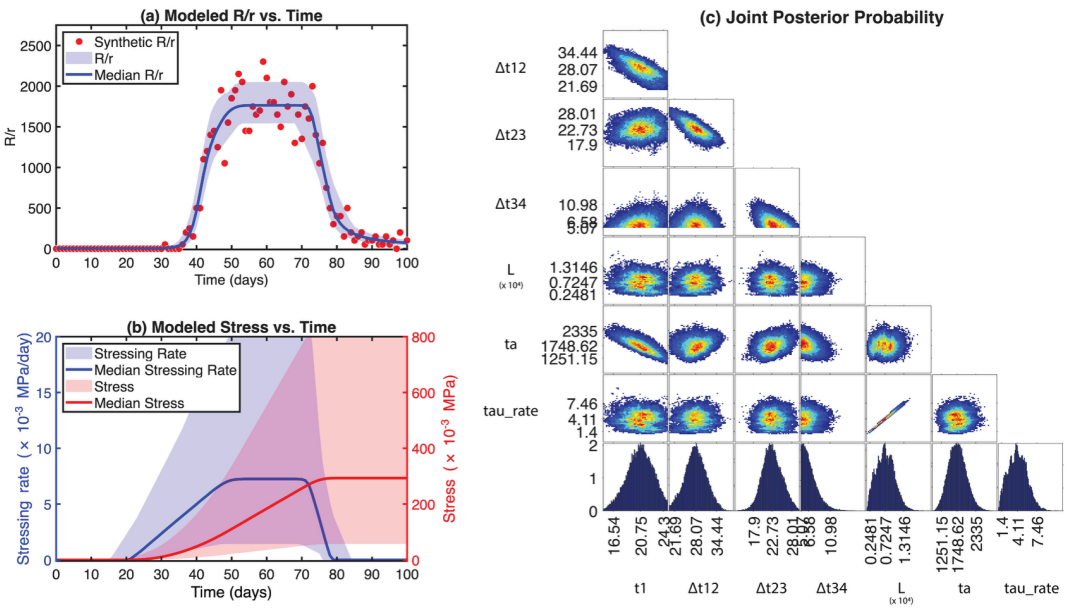

Figure 1. Input data and inversion results for the synthetic control experiment. (a) modeled *R*/*r*, (b) modeled stressing rate and stress, and (c) joint posterior probability.

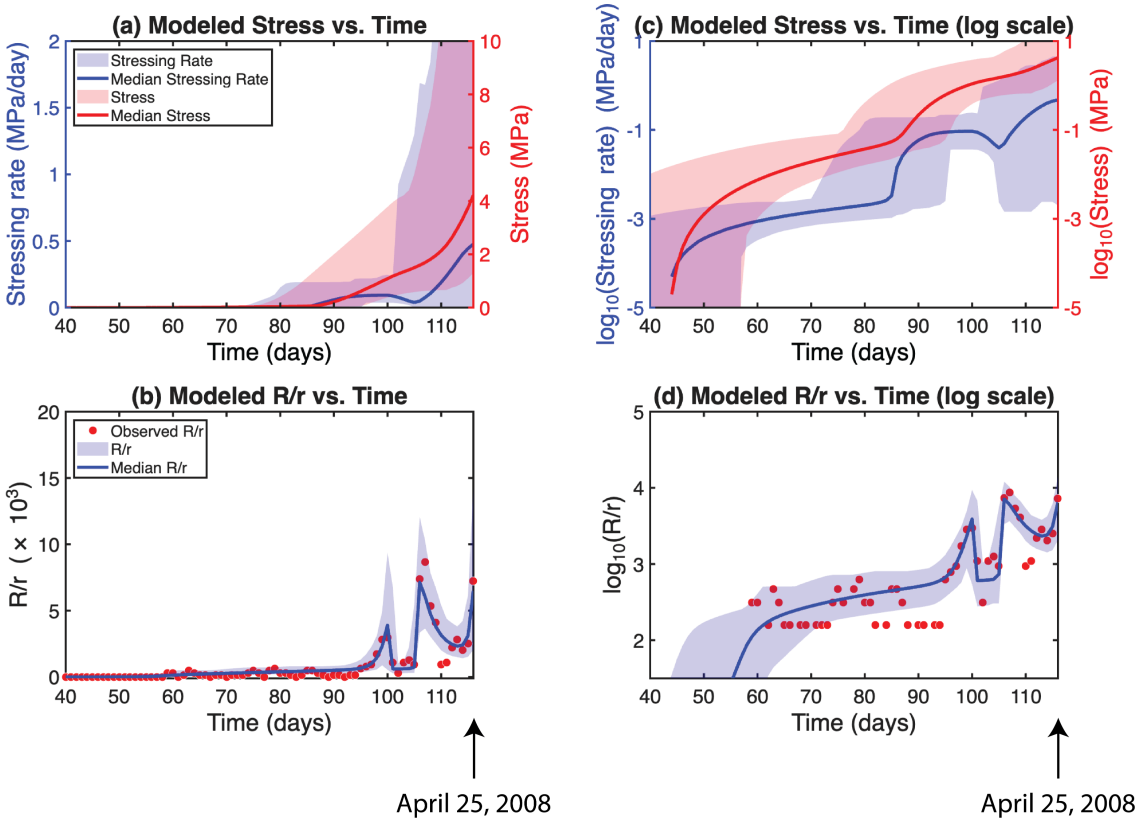

Figure 2. Stress and seismicity rate analysis of the 2008 Reno-Mogul, Nevada, swarm. (a) Modeled stress rate and stress are shown in blue lines and red lines; (c) is the same as (a) but

stress rate and stress in the logarithm scale. (b) Observed and modeled seismicity rates are shown in red circles and blue lines respectively; (d) is the same as (b) but the seismicity rate is in the logarithm scale. The x-axis represents the number of days since January 1, 2008. The last day on the x-axis is April 25, 2008, one day before April 26 when the M 5.1 occurred.

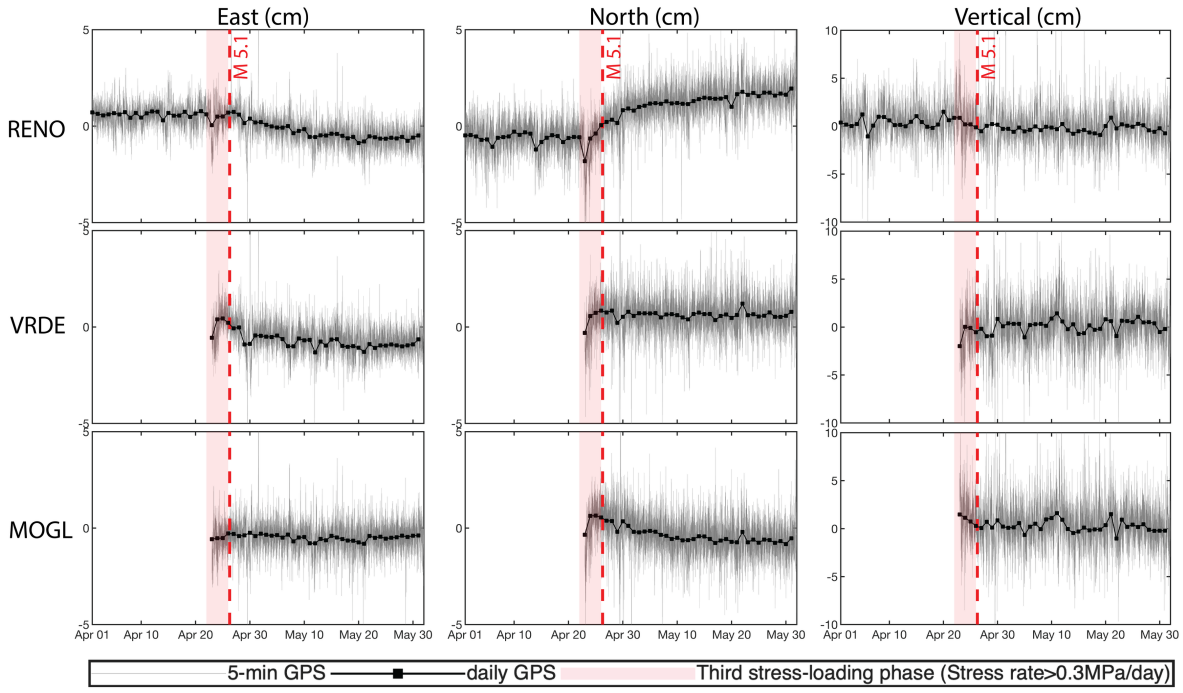

Figure 3. Time-series GPS observations during the 2008 Reno-Mogul earthquake swarm for three stations: RENO, VRDE and MOGL. Grey lines show the 5-min GPS data, and black squares show the daily GPS data. The red dashed line indicates the time when the M5.1 earthquake occurred. The pink shaded zone indicated the stress rate higher than 0.3 MPa/day during third stress-loading phase based on the seismicity rate inversion shown in Figure 2.

Presentations

Jiang, Y., Trugman, D. & González, P. (2025). Bayesian inference of stress evolution in rate-and-state governed faults constrained by seismicity rate observations. Poster Presentation at 2025 SSA Annual Meeting.

Jiang, Y., & Trugman, D. (2025). Examining precursory stress changes during earthquake swarms in California and Nevada from seismicity rate observations. Poster Presentation at 2025 SCEC Annual Meeting.

Articles under review

Jiang, Y., Trugman, D. & González, P. Bayesian inference of complex stress evolution in rate-and-state governed faults constrained by seismicity rate observations. *Journal of Geophysical Research - Solid Earth* (in review).

References

Abril-Pla, O., Andreani, V., Carroll, C., Dong, L., Fonnesbeck, C. J., Kochurov, M., Kumar, R., Lao, J., Luhmann, C. C., Martin, O. A., Osthege, M., Vieira, R., Wiecki, T., & Zinkov, R. (2023). PyMC: a modern, and comprehensive probabilistic programming framework in Python. PeerJ Computer Science, 9, e1516. https://doi.org/10.7717/PEERJ-CS.1516

Dieterich, J. (1994). A constitutive law for rate of earthquake production and its application to earthquake clustering. Journal of Geophysical Research, 99(B2), 2601-2618. https://doi.org/10.1029/93JB02581

Heimisson, E. R., & Segall, P. (2018). Constitutive Law for Earthquake Production Based on Rate-and-State Friction: Dieterich 1994 Revisited. Journal of Geophysical Research: Solid Earth, 123(5), 4141-4156. https://doi.org/10.1029/2018JB015656

Segall, P., Desmarais, E. K., Shelly, D., Miklius, A., & Cervelli, P. (2006). Earthquakes triggered by silent slip events on Kīlauea volcano, Hawaii. Nature, 442(7098), 71-74. https://doi.org/10.1038/NATURE04938

Sirorattanakul, K., Ross, Z. E., Khoshmanesh, M., Cochran, E. S., Acosta, M., & Avouac, J.-P. (2022). The 2020 Westmorland, California earthquake swarm as aftershocks of a slow slip event sustained by fluid flow. Journal of Geophysical Research: Solid Earth, 127, e2022JB024693. https://doi.org/10.1029/2022JB024693

Zaliapin, I., & Ben-Zion, Y. (2013). Earthquake clusters in southern California I: Identification and stability. Journal of Geophysical Research: Solid Earth, 118(6), 2847-2864. https://doi.org/10.1002/JGRB.50179

Zaliapin, I., & Ben-Zion, Y. (2020). Earthquake Declustering Using the Nearest-Neighbor Approach in Space-Time-Magnitude Domain. Journal of Geophysical Research: Solid Earth, 125(4), e2018JB017120. https://doi.org/10.1029/2018JB017120